Radiative transfer on curved surfaces

J. Tessendorf
Climate System Research Program, College of Geosciences, Texas A&M University, College Station, Texas 77843

(Received 26 April 1989; accepted for publication 15 November 1989)

After a review of appropriate concepts in local surface geometry, a formally exact solution of the radiative transfer equation is constructed, for transfer from one surface of arbitrary shape to another. The solution is obtained from repeated application of the linear interaction principle to form a path integral over paths that cross many intermediate surfaces. Invariant imbedding in general geometries is presented and found to be manifest in the path integral solution as an invariance under local coordinate transformations of the intermediate surfaces. Aspects of possible numerical implementations of this geometrical approach are discussed.

I. INTRODUCTION

There are a number of problems of current interest in atmospheric remote sensing and ocean optics that have the common need for knowledge of the distribution of radiation propagated through a medium with curved or irregular boundaries. One such problem is the conversion of measured brightness temperatures of clouds into an estimate of the local rain rate,[1,2] in which the microwave emission by rainfall suffers absorption and multiple scattering in the volume of rain, ice particles, and cloud liquid water content. Plane-parallel models of rain fields with finite horizontal extent, for example, show that the brightness temperature–rain rate connection is significantly affected by the spatial extent of the rain field.[3]

There is a very active effort to calculate the radiance distribution emitted and reflected by clouds in the visible and IR regimes. Some Monte Carlo calculations have been used to study the effects of cloud geometry,[4] and a multimode technique exists for geometries that can be represented by a collection of cuboids.[5] The cloud geometry is more important in these regimes than in the microwave emission problem, because the cloud body itself is more attenuating in the visible and IR than at microwave wavelengths.

The resolution of underwater imaging systems is limited by blurring and contrast reduction, induced by scattering and absorption in the water. These effects can be suppressed somewhat by removal of the corresponding Mutual Transfer Function (MTF) from the image, or by range-gating the transceiver system.[6–8] Typically the formulation of the underwater imaging problem treats the imaged object as lying in a plane parallel to the camera plane. When the object has an extended structure within the field of view, however, it may be necessary to accommodate the range of scattering and absorption within the image by accounting for the object's three-dimensional shape.

These three examples illustrate radiative transfer problems with complicated spatial boundaries. In the first two examples the medium itself is bounded by irregular surfaces (the source of radiant power also has irregular bounds), while in the third the reflecting surface has some three-dimensional shape and the medium is effectively unbounded (ignoring for the moment any effects of the ocean surface in altering the light field). The geometric aspects of these examples are as important as the scattering and absorbing properties of the media. In general, any radiative transfer problem that involves an inhomogeneous medium and/or boundaries exhibits sensitivity to the geometry.

It seems worthwhile, therefore, to frame the solution of the radiative transfer equation in terms of the appropriate geometrical setting. This has been carried out in great detail and rigor for the special case of a medium composed of parallel planes, under the elegant formalism of reflection and transmission operators[9,10] in the context of the invariant imbedding relations. Preisendorfer also developed the full invariant imbedding relations for arbitrarily shaped media,[11] but, in that case, the emphasis was on developing relations with structure analogous to the flat surface case, and the geometric aspects were left implicit.

The purpose of this paper is to clarify the role of surface geometry in the solution of the radiative transfer equation and in the invariant imbedding relations. The approach taken is to construct an evolution operator for the general solution of the radiative transfer equation. In this way problems with constrained boundary conditions are restated as evolution problems with constrained initial conditions, and it is this latter form of the solution that yields most directly the invariant imbedding relations. A brief review is provided in Sec. III of invariant imbedding on flat surfaces, along with a generalization to curved surfaces.

The evolution operator approach has been used a number of times,[9,12,13] each distinguished by its own particular variations. In their basic form all of the variations assume the distribution is known on an initial plane, or assume complementary partial information on several planes, and use the evolution operator or transmission and reflection operators to obtain the distribution on the final plane(s) of interest. The more recent references construct the evolution operator in terms of a path integral[12] or a discretized matrix operator.[13] The two are related in the sense that the path integral solution is obtained in the limit of a very fine discretization for the matrix quantities.

However, as mentioned above, it is desirable to generalize the bounding planes to curved surfaces with potentially very complicated structure. The parametrization of the me-

 0022-2488/90/041010-10$03.00

dium in terms of curved surfaces is accomplished in Sec. II. The linear interaction principle is used to begin the construction of the evolution operator in Sec. III. The result is the evolution operator for the transfer of radiance from the initial surface to the final surface, obtained from a sequence of transfers across many intermediate surfaces. When a large number of intermediate surfaces is used, the evolution operator for each transfer becomes an infinitesimal operator. The infinitesimal evolution operator is constructed in Sec. IV using the radiative transfer equation, and the full expression for the evolution operator in terms of a path integral is obtained. The path integral method for constructing the evolution operator has been used in the context of ocean optics,[12,14,15] and much of the notation and techniques used below can be found there.

One interesting consequence of incorporating surface geometry into the path integral formalism is that the principle of invariant imbedding is the natural consequence of the fact that the formal expression for the evolution operator is invariant under arbitrary local coordinate transformations of the intermediate surfaces. This invariance is demonstrated in Sec. V.

In Sec. VI, the explicit inclusion of the surface geometry is discussed as a possible method of improving the efficiency of numerical algorithms (such as finite-difference) that employ a spatial grid mesh.

The notation used below for the radiative transfer equation is

$$\{\hat{n}\cdot\nabla + c\}L(\mathbf{x},\hat{n}) = \int d\Omega'\,\beta(\hat{n}\cdot\hat{n}')L(\mathbf{x},\hat{n}'),$$

where L is the radiance, $\mathbf{x}$ is the position in the volume, $\hat{n}$ is the direction of propagation, c is the total extinction coefficient, and β is the volume scattering function. The dependence of the optical properties c and β on position in the volume is ignored, although all of the results can be extended to include a nonhomogeneous medium. For convenience, the volume scattering function is written as

$$\beta(\hat{n}\cdot\hat{n}') = b\,P(\hat{n}\cdot\hat{n}'),$$

where b is the scattering coefficient,

$$b = \int d\Omega\,\beta(\hat{n}\cdot\hat{n}'),$$

and the phase function P has unit normalization

$$\int d\Omega\,P(\hat{n}\cdot\hat{n}') = 1.$$

II. PARAMETRIZATION OF THE CURVED GEOMETRY

Suppose the volume of the medium is bounded by the two surfaces s_i and s_f, as in Fig. 1. Let $u \equiv (u^a) \equiv (u^1,u^2)$ be coordinates of a two-dimensional plane. A point $\mathbf{x}(u)$ on a surface is a mapping of a point u of the 2-D plane to the surface in the 3-D volume, indicated in Fig. 1 by the shape of the (u^1,u^2) mesh on the surface. All points in the volume of the medium can be parametrized by introducing the label s for each surface. The surface $s = s_i$ is the surface on which the distribution is known, and $s = s_f$ is the surface on which the distribution is to be obtained. The volume between these

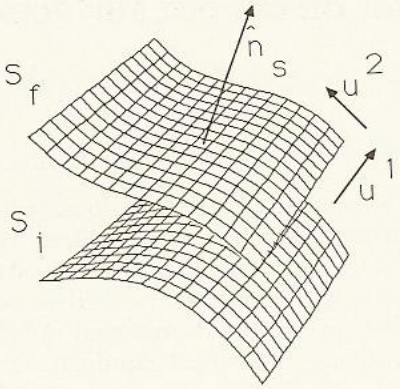

FIG. 1. Surface geometry showing (u^1,u^2) coordinates, surface normal, and layer of initial and final surfaces s_i, s_f.

surfaces is the layered set of surfaces $s_i \leqslant s \leqslant s_f$. Each point in the volume is uniquely labeled by a triplet (u,s) with s labeling the particular surface, and u labeling the position on the surface. Points in the volume can be denoted $\mathbf{x}(u,s)$.

Several concepts and quantities from differential geometry come into the formal calculations below (Ref. 16 is a good source). The primary quantity is the metric g. For a fixed surface s, the metric with components g_{ab} is defined as

$$g_{ab}(u,s) = \mathbf{x}_a(u,s)\cdot\mathbf{x}_b(u,s),$$

where $\mathbf{x}_a$ is

$$\mathbf{x}_a = \frac{\partial}{\partial u^a}\mathbf{x}.$$

The metric considered as a matrix has an inverse whose components are denoted g^{ab}, and which satisfies (implied summation over repeated indices is used throughout)

$$g_{ab}g^{bc} = g^{cb}g_{ba} = \delta_a^c,$$

where δ_a^c is the Kronecker delta function.

The two vectors $\mathbf{x}_a(u,s)$ define the local tangent plane to the surface, and are orthogonal to the surface normal (although they are not necessarily orthogonal to each other). The surface normal can be constructed from the cross product of the tangent vectors:

$$\hat{n}_s(u,s) = \frac{\mathbf{x}_1(u,s)\times\mathbf{x}_2(u,s)}{|\mathbf{x}_1(u,s)\times\mathbf{x}_2(u,s)|}.$$

A third vector defined at each point is $\dot{\mathbf{x}}(u,s)$, where, for convenience, derivatives with respect to s are denoted by

$$\dot{\mathbf{x}} \equiv \frac{\partial}{\partial s}\mathbf{x}.$$

Although this vector at each point on the surface is not necessarily orthogonal to either $\mathbf{x}_1$ or $\mathbf{x}_2$, it does not lie in the tangent plane, since it describes the layering of surfaces in the volume. Therefore the set of three vectors $\{\mathbf{x}_1, \mathbf{x}_2, \dot{\mathbf{x}}\}$ could be used to construct a local basis of the three-dimensional space. However, as will be clear below, it is more convenient to use a basis in which $\dot{\mathbf{x}}$ is replaced by its component $\dot{\mathbf{x}}_\perp$ orthogonal to the tangent plane, given by

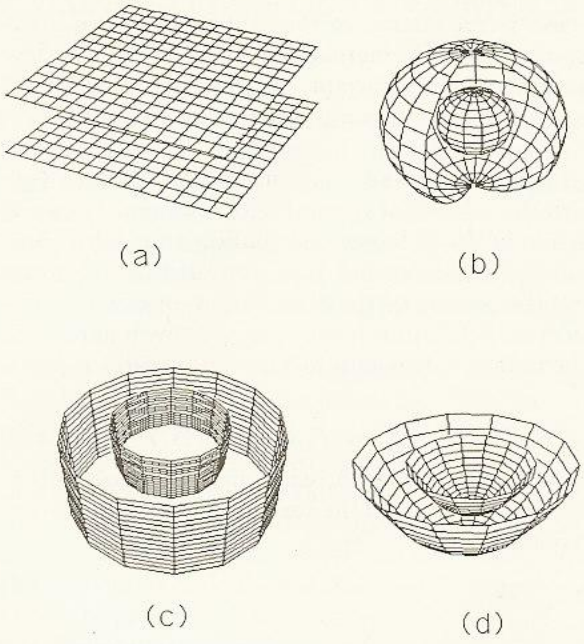

FIG. 2. Example volumes parametrized as layers of surfaces. (a) Layered flat planes; (b) imbedded concentric spheres; (c) imbedded concentric cylinders; (d) translated Monge patches.

$$\dot{\mathbf{x}}_\perp = \dot{\mathbf{x}} - f^a \mathbf{x}_a,$$

where

$$f^a = g^{ab}(\mathbf{x}_b \cdot \dot{\mathbf{x}}).$$

It can be verified directly from this definition that $\mathbf{x}_b \cdot \dot{\mathbf{x}}_\perp = 0$, and so $\dot{\mathbf{x}}_\perp$ is parallel to the surface normal, and we may write

$$\hat{n}_s(u,s) = \dot{\mathbf{x}}_\perp(u,s)/|\dot{\mathbf{x}}_\perp(u,s)|.$$

The local three-dimensional basis used below is the set of vectors $\{\mathbf{x}_1,\mathbf{x}_2,\dot{\mathbf{x}}_\perp\}$.

As examples of this description of local geometry, we consider four examples illustrated in Fig. 2: layered flat planes, imbedded concentric spheres, imbedded concentric cylinders, and translated Monge patches. Each example is discussed below, and summarized in Table I.

Layered flat planes: Using the Cartesian coordinates (x,y,z), we take $u = (x,y)$ and $s = z$. Points $\mathbf{x}$ on each plane are given by $\mathbf{x} = (x,y,z)$, so that the basis $\{\mathbf{x}_1,\mathbf{x}_2,\dot{\mathbf{x}}_\perp\}$ is just the orthonormal set $\{(1,0,0), (0,1,0), (0,0,1)\}$.

Imbedded concentric spheres: Using the spherical coordinates (r,θ,ϕ), we assign $s = r$, and $u = (\theta,\phi)$. Positions on the surface of constant radius r are

$$\mathbf{x} = (r\sin\theta\cos\phi, r\sin\theta\sin\phi, r\cos\theta).$$

The derivative vectors are

$$\dot{\mathbf{x}} = (\sin\theta\cos\phi, \sin\theta\sin\phi, \cos\theta),$$

$$\mathbf{x}_1 = (r\cos\theta\cos\phi, r\cos\theta\sin\phi, -r\sin\theta),$$

$$\mathbf{x}_2 = (-r\sin\theta\sin\phi, r\sin\theta\cos\phi, 0).$$

The metric is

$$[g_{ab}] = r^2\begin{bmatrix} 1 & 0 \\ 0 & \sin^2\theta \end{bmatrix}.$$

The perpendicular component of $\dot{\mathbf{x}}$ is

$$\dot{\mathbf{x}}_\perp = (\sin\theta\cos\phi, \sin\theta\sin\phi, \cos\theta),$$

and this is also the surface normal $\hat{n}_s$.

Imbedded concentric cylinders: The cylindrical coordinates (ρ,φ,z) are assigned as $s = \rho$, $u = (\varphi,z)$. Positions on the surface of constant radius ρ are

$$\mathbf{x} = (\rho\cos\varphi, \rho\sin\varphi, z).$$

The derivative vectors are

$$\dot{\mathbf{x}} = (\cos\varphi, \sin\varphi, 0),$$

$$\mathbf{x}_1 = (-\rho\sin\varphi, \rho\cos\varphi, 0),$$

$$\mathbf{x}_2 = (0,0,1).$$

The metric is

$$[g_{ab}] = \begin{bmatrix} \rho^2 & 0 \\ 0 & 1 \end{bmatrix},$$

and the perpendicular component of $\dot{\mathbf{x}}$ is

$$\dot{\mathbf{x}}_\perp = (\cos\varphi, \sin\varphi, 0) = \hat{n}_s.$$

Translated Monge patches: A Monge patch is a surface of the form

$$\mathbf{x} = (x,y,h(x,y)),$$

where h is some well-behaved function and (x,y) are Cartesian coordinates. We can construct a volume by translating the Monge patch in the vertical direction, so that each Monte patch is given by $s = \text{const}$, and

$$\mathbf{x}(x,y,s) = (x,y,h(x,y) + s).$$

TABLE I. Summary of the example geometry coordinate systems.

	u^1	u^2	s	$\mathbf{x}$	$\dot{\mathbf{x}}$	$\mathbf{x}_1$	$\mathbf{x}_2$	$\dot{\mathbf{x}}_\perp$
Plane	x	y	z	(x,y,z)	$(0,0,1)$	$(1,0,0)$	$(0,1,0)$	$(0,0,1)$
Sphere	θ	ϕ	r	$(r\sin\theta\cos\phi, r\sin\theta\sin\phi, r\cos\theta)$	$(\sin\theta\cos\phi, \sin\theta\sin\phi, \cos\theta)$	$(r\cos\theta\cos\phi, r\cos\theta\sin\phi, -r\sin\theta)$	$(-r\sin\theta\sin\phi, r\sin\theta\cos\phi, 0)$	$(\sin\theta\cos\phi, \sin\theta\sin\phi, \cos\theta)$
Cylinder	φ	z	ρ	$(\rho\cos\varphi, \rho\sin\varphi, z)$	$(\cos\varphi, \sin\varphi, 0)$	$(-\rho\sin\varphi, \rho\cos\varphi, 0)$	$(0,0,1)$	$(\cos\varphi, \sin\varphi, 0)$
Monge patch	z	y	s	$(x,y,h(x,y) + s)$	$(0,0,1)$	$(1,0,h_x)$	$(0,1,h_y)$	$(-h_x, -h_y, 1)$

We take $u = (x,y)$, and the derivative vectors are

$$\dot{\mathbf{x}} = (0,0,1), \quad \mathbf{x}_1 = (1,0,h_x), \quad \mathbf{x}_2 = (0,1,h_y).$$

The metric is

$$[g_{ab}] = \begin{bmatrix} 1+h_x^2 & h_x h_y \\ h_x h_y & 1+h_y^2 \end{bmatrix},$$

and the perpendicular component of $\dot{\mathbf{x}}$ is

$$\dot{\mathbf{x}}_\perp = (-h_x, -h_y, 1).$$

The surface normal is

$$\hat{n}_s = (-h_x, -h_y, 1)/(1+h_x^2+h_y^2)^{1/2}.$$

These examples are used in the sections below to illustrate the geometric structure of the evolution operator.

III. THE EVOLUTION OPERATOR AND INVARIANT IMBEDDING

A functional definition for the evolution operator G can now be made. It is convenient to write G in the form $G(u,s_f,\hat{n};u',s_i,\hat{n}')$, and it is implicitly a function of the points on each of the two surfaces, and the intervening points. In this form the solution of the radiative transfer equation at points on the surface s_f is

$$L(\mathbf{x}(u,s_f),\hat{n}) = \int d^2u'\, d\Omega'\, G(u,s_f,\hat{n};u',s_i,\hat{n}') \times L(\mathbf{x}(u',s_i),\hat{n}'). \tag{1}$$

For this solution the evolution operator must satisfy the radiative transfer equation with the initial condition

$$G(u,s_f,\hat{n};u',s_i,\hat{n}')|_{i\to f} = \delta(u-u')\delta(\hat{n}-\hat{n}').$$

The operator G is an evolution operator because, according to the linear interaction principle, it can be constructed from intermediate solutions. Suppose a particular intermediate surface s_1 between s_i and s_f is chosen. Using G, the radiance distribution at this intermediate surface is

$$L(\mathbf{x}(u,s_1),\hat{n}) = \int d^2u'\, d\Omega'\, G(u,s_1,\hat{n};u',s_i,\hat{n}') \times L(\mathbf{x}(u',s_i),\hat{n}').$$

Using the distribution at this intermediate surface, the distribution at the final surface s_f is

$$L(\mathbf{x}(u,s_f),\hat{n}) = \int d^2u'\, d\Omega'\, G(u,s_f,\hat{n};u',s_1,\hat{n}') \times L(\mathbf{x}(u',s_1),\hat{n}').$$

Combining these two results with the expression in Eq. (1), the operator G satisfies the convolution relationship

$$G(u,s_f,\hat{n};u_i,s_i,\hat{n}') = \int d^2u''\, d\Omega'' \times G(u,s_f,\hat{n};u'',s_1,\hat{n}'')\, G(u'',s_1,\hat{n}'';u',s_i,\hat{n}'). \tag{2}$$

An alternate method of constructing a solution to the radiative transfer equation employs information about the radiance distribution on two parallel planes to obtain the distribution between them, using transmission and reflection operators. This method leads to the invariant imbedding principle, and is the source of the adding–doubling algorithm in some numerical methods of solution.[5] We review briefly this form of the invariant imbedding principle, and discuss how it is modified in a more general geometric setting.

Suppose surfaces s_1 and s_2 are flat parallel planes (see Fig. 3), with the normal of s_1 pointing ("upward") toward s_2. The portion of the radiance distribution on s_1 with components parallel to the normal (i.e., "upward") is denoted $L_U(s_1)$, and the portion of the distribution on s_2 with components antiparallel to the normal (i.e., "downward") is $L_D(s_2)$. The radiance distribution between s_1 and s_2 is given by

$$L(s) = F_U(s,s_1)L_U(s_1) + F_D(s,s_2)L_D(s_2), \tag{3}$$

where (F_U,F_D) are the transmission and reflection operators, and we have suppressed the surface and angular convolutions. Explicitly,

$$F_{U,D}(s,s_i)L_{U,D}(s_i) \equiv \int d^2u' \int_{U,D} d\Omega' \times F_{U,D}(u,s,\hat{n};u',s_i,\hat{n}')L_{U,D}(u',s_i,\hat{n}'),$$

and the angular integrations are restricted to just the upward or downward direction, as appropriate. Equation (3) is the invariant imbedding equation. Its fundamental importance is that the radiance distribution on any plane s is determined by the distribution on the initial planes s_1 and s_2, but not by how the region between s_1 and s_2 is represented.

This solution can be iterated by choosing two planes s_3 and s_4, such as those shown in Fig. 3. From Eq. (3),

$$L(s_3) = F_U(s_3,s_1)L_U(s_1) + F_D(s_3,s_2)L_D(s_2),$$
$$L(s_4) = F_U(s_4,s_1)L_U(s_1) + F_D(s_4,s_2)L_D(s_2).$$

We can also write the invariant imbedding equation just in terms of the s_3 and s_4 surfaces:

$$L(s) = F_U(s,s_3)L_U(s_3) + F_D(s,s_4)L_D(s_4).$$

Denoting the upward component of F_U by F_{UU}, the downward component by F_{UD}, etc., we obtain

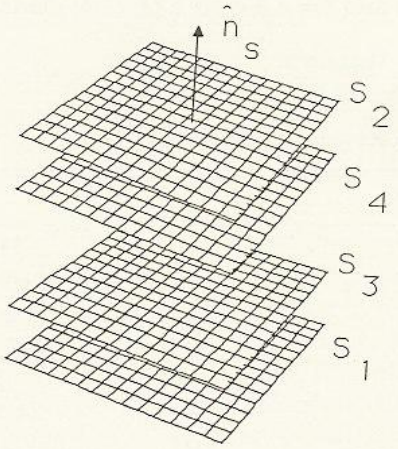

FIG. 3. Planar geometry used to describe the invariant imbedding principle.

$$F_U(s,s_1) = F_U(s,s_3)F_{UU}(s_3,s_1) + F_D(s,s_4)F_{UD}(s_4,s_1),$$
$$F_D(s,s_2) = F_U(s,s_3)F_{DU}(s_3,s_2) + F_D(s,s_4)F_{DD}(s_4,s_2). \quad (4)$$

Although this is an expression for $F_U(s,s_1)$ and $F_D(s,s_2)$ in terms of transmission and reflection operators at the intermediate planes s_3 and s_4, recall that s_3 and s_4 were introduced as convenient surfaces on which to iterate the invariant imbedding equation. The original solution is independent of any particular intermediate planes. Thus the invariant imbedding equation allows us to introduce additional conveniently located planes imbedded between s_1 and s_2, but guarantees that the solution obtained from such a decomposition is independent of the chosen imbedding. In Sec. V, this result is generalized to allow the imbedded surfaces to have arbitrary shape as well.

Despite the manipulations used above, the invariant imbedding principle can be stated in a simple, physically intuitive way: given a medium partitioned into regions, the operators in the full volume can be built up from the operators in the individual regions, and the result is independent of the choice of partition of the medium.

Preisendorfer considered the invariant imbedding problem in more general geometries. The basic change in the formalism arises from the fact that there is no longer a unique up and down orientation as in the planar geometry. Instead, up and down are defined locally according to the direction of the surface normal at each point. However, it should be possible to construct the invariant imbedding equation without choosing particular orientations. The necessity of the up and down directionality arises from the choice of the initial condition problem: the known distributions are $L_U(s_1)$ and $L_D(s_2)$, and so the problem is phrased in terms of these up and down directions.

We can, however, phrase a new problem: Suppose $\{s_1,\ldots,s_N\}$ is a set of surfaces on which the radiance distribution $L(s_j)$ is known. We wish to find a solution $L(s)$ in the rest of the medium. From the linear interaction principle or the general form of the invariant imbedding equation, we might expect to write the solution as

$$L(s) = \sum_{j=1}^{N} F(s,s_j)L(s_j),$$

with

$$F(s_k,s_j) = \delta_{jk},$$

but we do not know yet what the F's are. Note that each of

$$L_j(s) = G(s,s_j)L(s_j),$$

are solutions of the radiative transfer equation, with $L_j(s_j) = L(s_j)$, but that the sum of these does not satisfy the conditions on each of the surfaces. However, a general solution using the evolution operator can be written

$$L(s) = \int ds'\, G(s,s')H(s').$$

The task is to find a function H that satisfies the initial condition on each surface. An ansatz for the solution is

$$H(s') = \sum_{j=1}^{N} \delta(s' - s_j)A_jL(s_j),$$

where the A_j are operators:

$$H(u,s,\hat{n}) = \sum_{j=1}^{N} \delta(s - s_j)\int d^2u'\, d\Omega' \times A_j(u,\hat{n};u',\hat{n}')L(u',s_j,\hat{n}').$$

The solution is found if the operators A_j satisfy the equation

$$\sum_j (G(s_k,s_j)A_j - \delta_{kj})L(s_j) = 0.$$

This is just the requirement that the functional determinant vanish:

$$\mathrm{Det}(G(s_k,s_j)A_j - \delta_{kj}) = 0.$$

Thus the A_j are related to the eigenvalues of $G(s_k,s_j)$. It is unclear under what conditions the A_j fail to exist. Presumably some choices of distributions and surfaces are incompatible, and a solution cannot exist. On the other extreme, we can reduce the geometry to the flat plane case discussed above, and only specify the appropriate up and down components, for which the solution is known to exist. The transition between these extremes is not understood, however.

Assuming for the moment the A_j exist, the solution is

$$L(s) = \sum_j G(s,s_j)A_jL(s_j),$$

which is the invariant imbedding equation with $F(s,s_j) = G(s,s_j)A_j$.

IV. CONSTRUCTION OF THE PATH INTEGRAL REPRESENTATION

The path integral representation constructed below follows from the linear interaction principle by iterating Eq. (2) over many intermediate surfaces. Suppose there are $N+1$ surfaces s_j, $j = 0,\ldots,N$, with $s_0 = s_i$ and $s_N = s_f$; then successive iterations of Eq. (2) produce the result

$$G(u_f,s_f,\hat{n}_f;\, u_i,s_i,\hat{n}_i) = \int \prod_{j=1}^{N-1} d^2u_j\, d\Omega_j \times \prod_{j=1}^{N} G(u_j,s_j,\hat{n}_j;\, u_{j-1},s_{j-1},\hat{n}_{j-1}). \quad (5)$$

In the limit $N \to \infty$, this expression becomes the path integral representation.

To aid in understanding the path integral representation, we can think of G in terms of an effective attenuation coefficient τ_{eff} for an arbitrary path that starts at s_i and ends at s_f, summed over all such paths[12]:

$$G(s_f,s_i) \sim \sum_{\mathrm{path}} \exp\{-\tau_{\mathrm{eff}}(\mathrm{path})\}.$$

Loosely speaking, when the number of intermediate surfaces N is large,

$$G(s_j,s_{j-1}) \sim \exp\{-\tau_{\mathrm{eff}}(s_j,s_{j-1})\},$$

so that

$$\tau_{\mathrm{eff}}(\mathrm{path}) \sim \sum_j \tau_{\mathrm{eff}}(s_j,s_{j-1}).$$

This statement is not rigorous, although it can be a useful way of picturing the physical content of the path integral. It is rigorous, however, to write

$$G(s_j,S_{j-1}) = \exp\{-\tau_c(s_j,s_{j-1})\}G_{\text{scatt}}(s_j,s_{j-1})$$

in the limit $N\to\infty$, in which τ_c accounts for total extinction, and G_{scatt} accounts for the distribution of scattering. Analogous to the construction of the evolution operator in quantum mechanics, a phase space is introduced below combining the set of all paths with the set of all directional modes of scattering at each point on a path, to yield a rigorous construction

$$G(s_f,s_i) = \sum_{\text{configurations}} \exp\{-\tau_{\text{eff}}(\text{configuration})\},$$

where $\Sigma_{\text{configurations}}$ means the sum over all phase space configurations of paths.

The first step in the construction is to parametrize an arbitrary path in the medium. This amounts to tracing a ray from the initial surface to the final surface, with its position on surface s denoted $\mathbf{l}(s)$. The local tangent of the path is a unit vector $\hat{\beta}$ pointing in the direction of propagation along the path, and is defined as[16]

$$\hat{\beta}(s) = \frac{d\mathbf{l}(s)/ds}{|d\mathbf{l}(s)/ds|}.$$

Alternatively, we can write this relationship in the differential form

$$d\mathbf{l}(s) = dl(s)\hat{\beta}(s).$$

The path $\mathbf{l}$ and its differential elements $d\mathbf{l}$ have been parametrized just in terms of the surface label s, without the use of the surface coordinates u. However, for the purpose of construction of the path integral representation, it is convenient to describe the path in terms of the local tangent vector $\hat{\beta}(s)$, and the points $\mathbf{l}(s_i)$ and $\mathbf{l}(s_f)$ on the initial and final surfaces. Thus we treat $\hat{\beta}(s)$ as the prescribed quantity of a path, and find an expression for the position along the path in terms of the surface coordinates u. Recalling that the triplet $\{\mathbf{x}_1, \mathbf{x}_2, \dot{\mathbf{x}}_\perp\}$ forms a local basis, the differential $d\mathbf{l}$ can be decomposed as (see Figs. 4 and 5)

$$\begin{aligned} d\mathbf{l} &= dl\hat{\beta} \\ &= \dot{\mathbf{x}}\,ds + \dot{\mathbf{x}}_a\,du^a \\ &= \dot{\mathbf{x}}_\perp\,ds + f^a\mathbf{x}_a\,ds + \mathbf{x}_a\,du^a. \end{aligned}$$

Because $\dot{\mathbf{x}}_\perp$ is normal to the local tangent plane, the distance traveled between s and $s+ds$ is

$$dl = [|\dot{\mathbf{x}}_\perp|/(\hat{\beta}\cdot\hat{n}_S)]ds. \tag{6}$$

This expression is obtained by taking the inner product of $d\mathbf{l}$ with $\dot{\mathbf{x}}_\perp$.

Taking the inner product with $\mathbf{x}_a$ and using the result for dl, du^a satisfies the constraint

$$du^a = \{(\mathbf{x}^a\cdot\hat{\beta})[|\dot{\mathbf{x}}_\perp|/(\hat{\beta}\cdot\hat{n}_S)] - f^a\}\,ds, \tag{7}$$

where $\mathbf{x}^a$ is related to $\mathbf{x}_a$ by

$$\mathbf{x}^a = g^{ab}\mathbf{x}_b,$$

and summation over the repeated index is implied. This constraint equation for du^a can be converted to the nonlinear differential equation

$$\frac{du^a(s)}{ds} = (\mathbf{x}^a(u,s)\cdot\hat{\beta}(s))\frac{|\dot{\mathbf{x}}_\perp(u,s)|}{\hat{\beta}(s)\cdot\hat{n}_s(u,s)} - f^a(u,s) \tag{8}$$

describing the path in terms of the surface coordinates of a ray having the direction of propagation $\hat{\beta}(s)$ at each surface s. Table II is a list of the path equations for the example geometries.

The effective attenuation factor τ_{eff} has a contribution due to the total extinction coefficient c, and one due to the distribution of scattering described by the phase function. For a ray from surface s to $s+ds$, the total extinction is

$$\tau_c(s+ds,s) = c\,dl.$$

This expression is the straightforward consequence of the exponential character of total extinction.

The redistribution due to scattering is more difficult to obtain. However, the procedure used by Tessendorf[12,14] is the same as is needed here. Simply stating the result,

$$G_{\text{scatt}}(s+ds,s) \int_{-\infty}^{\infty} d^3p\,\exp\{i\,ds\,\mathbf{p}\cdot\dot{\hat{\beta}}(s) + b\,dl\,\Pi(\mathbf{p})\}, \tag{9}$$

where Π is the "pseudo-Fourier transform" of the phase function P:

$$P(\hat{n}\cdot\hat{n}') = \int \frac{d^3p}{(2\pi)^3}\Pi(\mathbf{p})\exp\{i\mathbf{p}\cdot(\hat{n}-\hat{n}')\}.$$

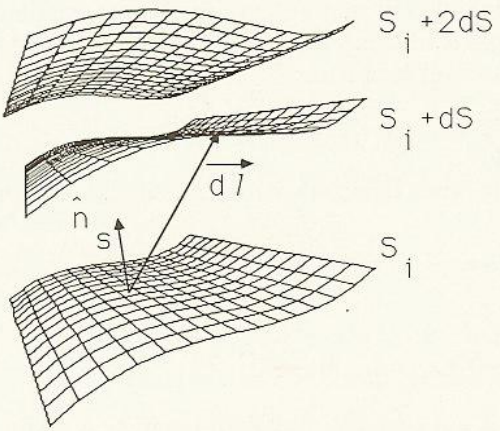

FIG. 4. Three-dimensional geometry showing the relationship between $\hat{n}_S$ and $d\mathbf{l}$.

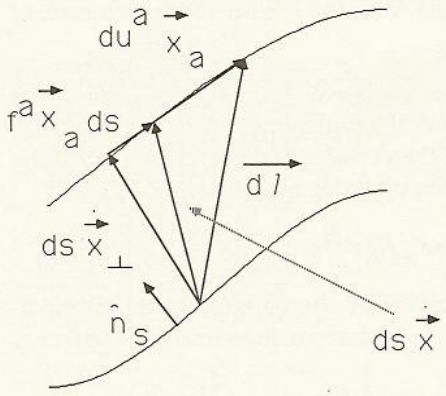

FIG. 5. The decomposition of $d\mathbf{l}$ in the $\{\mathbf{x}_1,\mathbf{x}_2,\dot{\mathbf{x}}_\perp\}$ basis.

TABLE II. Path equations for the example geometries.
$\hat{\beta}(s) = (\cos\epsilon(s)\sin\lambda(s), \sin\epsilon(s)\sin\lambda(s), \cos\lambda(s))$.

Layered flat planes
$\frac{dx}{dz} = \cos\epsilon\tan\lambda$
$\frac{dy}{dz} = \sin\epsilon\tan\lambda$
Imbedded concentric spheres
$\frac{d\theta}{dr} = \left(\frac{1}{r}\right)\frac{\tan\lambda\cos(\epsilon-\phi) - \tan\theta}{1+\tan\lambda\tan\theta\cos(\epsilon-\phi)}$
$\frac{d\phi}{dr} = \left(\frac{1}{r}\right)\frac{\tan\lambda\sin(\epsilon-\phi)}{\cos\theta + \tan\lambda\sin\theta\cos(\epsilon-\phi)}$
Imbedded concentric cylinders
$\frac{d\varphi}{d\rho} = \frac{1}{\rho}\tan(\epsilon-\varphi)$
$\frac{dz}{d\rho} = \cot\lambda\sec(\epsilon-\varphi)$
Translated Monge patches
$\frac{dx}{ds} = \frac{(1+h_y^2)\cos\epsilon\tan\lambda - h_x h_y\sin\epsilon\tan\lambda + h_x}{1 - h_x\cos\epsilon\tan\lambda - h_y\sin\epsilon\tan\lambda} - \frac{h_x}{1+h_x^2+h_y^2}$
$\frac{dy}{ds} = \frac{-h_x h_y\cos\epsilon\tan\lambda + (1+h_x^2)\sin\epsilon\tan\lambda + h_y}{1 - h_x\cos\epsilon\tan\lambda - h_y\sin\epsilon\tan\lambda} - \frac{h_y}{1+h_x^2+h_y^2}$

The term "pseudo" refers to the fact that the representation of P in terms of Fourier amplitudes Π cannot be inverted in the usual sense of Fourier transforms to provide a unique expression for Π. We can, however, define Π as the inverse Fourier transform of a function $\overline{P}$:

$$\Pi(\mathbf{p}) = \int d^3\sigma\,\overline{P}(\boldsymbol{\sigma})\exp\{-i\mathbf{p}\cdot\boldsymbol{\sigma}\}, \tag{10}$$

where, for $\sigma \leqslant 2$,

$$\overline{P}(\boldsymbol{\sigma}) = P(1-\sigma^2/2),$$

and, for $\sigma > 2$, $\overline{P}$ converges to zero sufficiently fast to ensure the existence of Eq. (10). For example, if we choose $\overline{P} = 0$ for $\sigma > 2$, then

$$\Pi(\mathbf{p}) = \frac{4\pi}{p}\int_0^2 \sigma\,d\sigma\sin(p\sigma)P\left(1-\frac{\sigma^2}{2}\right).$$

A similar approach for handling the phase function is used in the small-angle approximation of the radiative transfer equation.[17] This "pseudo-Fourier" representation is not restricted to small-angle problems, however, and is sufficiently general to include backscatter.

Note that the scattering contribution G_{scatt} has the form of an integral over the "scattering modes" $\mathbf{p}$. This brings about the introduction of the phase space, consisting of points $(\hat{\beta},\mathbf{p})$. The configurations described earlier are combinations of paths $\hat{\beta}(s)$ and scattering modes $\mathbf{p}(s)$ at each surface.

In addition to the attenuation factors from extinction and scattering, there must be in G an additional factor to enforce the ray-path constraint in Eq. (8). This can be included by setting

$$\begin{aligned} G(s+ds,s) &= \delta(\dot{u}^a(s) - (\mathbf{x}^a(u,s)\cdot\hat{\beta}(s)) \\ &\quad\times[\,|\dot{\mathbf{x}}_\perp(u,s)|/\hat{\beta}(s)\cdot\hat{n}_S(u,s)\,] + f^a(u,s)) \\ &\quad\times(1/ds)^2\exp\{-\tau_c(s+ds,s)\}G_{\text{scatt}}(s+ds,s). \end{aligned} \tag{11}$$

The full expression for G now follows from this expression placed in Eq. (5), in the limits $N\to\infty$ and $ds\to 0$ such that $N\,ds = s_f - s_i$. The notation for this solution is

$$\begin{aligned} G(u_f,s_f,\hat{n}_f;u_i,s_i,\hat{n}_i) &= \int (D\beta)(Du)(Dp)\delta(\hat{\beta}(s_i) - \hat{n}_i)\delta(\hat{\beta}(s_f) - \hat{n}_f) \\ &\quad\times\delta(u(s_i) - u_i)\delta(u(s_f) - u_f) \\ &\quad\times\prod_s \delta\left(\dot{u}^a - (\mathbf{x}^a\cdot\hat{\beta})\frac{|\dot{\mathbf{x}}_\perp|}{\hat{\beta}\cdot\hat{n}_S} + f^a\right) \\ &\quad\times\mathrm{Det}\left(\frac{\partial}{\partial s}\right)^2\exp\{-\tau_{\text{eff}}(\hat{\beta},\mathbf{p})\}. \end{aligned} \tag{12}$$

The integration measures $(D\beta)$, (Du), and (Dp) are

$$(D\beta) = \prod_s d\Omega(s),$$

$$(Du) = \prod_s d^2u(s),$$

$$(Dp) = \prod_s d^3p(s),$$

and the effective attenuation is

$$\begin{aligned} \tau_{\text{eff}}(\hat{\beta},\mathbf{p}) &= \int_{s_i}^{s_f} ds\,\frac{c|\dot{\mathbf{x}}_\perp|}{\hat{\beta}(s)\cdot\hat{n}_S} - i\int_{s_i}^{s_f} ds\,\mathbf{p}(s)\cdot\dot{\hat{\beta}}(s) \\ &\quad - \int_{s_i}^{s_f} ds\,b\Pi(\mathbf{p}(s))\frac{|\dot{\mathbf{x}}_\perp|}{\hat{\beta}(s)\cdot\hat{n}_S}. \end{aligned}$$

The constraint delta function introduced in Eq. (11) is a convenient method of obtaining the radiance distribution on each surface by following each path. The procedure for constraining integration variables in path integrals was introduced by Faddeev and Popov,[18] and it requires the inclusion of the factor

$$\mathrm{Det}\left(\frac{\partial}{\partial s}\right)^{-2}\mathrm{Det}\left\{\delta_{ab}\frac{\partial}{\partial s} - \frac{\delta}{\delta u^b}\left[(\mathbf{x}^a\cdot\hat{\beta})\frac{|\dot{\mathbf{x}}_\perp|}{\hat{\beta}\cdot\hat{n}_S} - f^a\right]\right\}.$$

Because the argument involves the first derivative in s, this term is equal to 1, and so is omitted. This was shown by Fried and Tessendorf in evaluation of a similar determinant in a fluid dynamics context.[19]

V. LOCAL COORDINATE TRANSFORMATIONS AND INVARIANT IMBEDDING

According to the invariant imbedding principle, the path integral expression for G should be independent of how the intermediate surfaces are parametrized. However, the

expression in Eq. (12) for G clearly uses an explicit parametrization of the intermediate surfaces. In fact, the path integral representation is independent of the parametrization, in the sense that local coordinate transformations can be performed on the surfaces, and the expression for G is left invariant. This invariance is demonstrated below.

A local coordinate transformation $u \to \bar{u}(u)$ on a surface is characterized by a transformation matrix Λ with components

$$\Lambda_b^a = \frac{\partial u^a}{\partial \bar{u}^b}.$$

A physical position $\mathbf{x}$ on a surface is not altered by a coordinate transforation, although the local tangent plane is now characterized by the transformed vectors

$$\bar{\mathbf{x}}_a = \Lambda_a^b \mathbf{x}_b.$$

This transformation follows from the chain rule for a change of variables. Transformation of the tangent plane vectors also transforms the metric:

$$\bar{g}_{ab} = \Lambda_a^c g_{cd} \Lambda_b^d.$$

It also follows that

$$\bar{\mathbf{x}}^a = (\Lambda^{-1})_b^a \mathbf{x}^b.$$

The second type of local coordinate transformation is a rescaling transformation of the surface labeling: $s \to \bar{s}(s)$. Note that this transformation preserves the order of the surface, since $s = \text{const}$ implies $\bar{s} = \text{const}$ also, but this transformation allows the density of the surfaces to be changed. We assume, however, that $\bar{s}$ is a monotonic function of s, so that the order of the surfaces is preserved.

We wish to examine the behavior of Eq. (12) under the most general transformation $(u,s) \to (\bar{u}(u,s),\bar{s}(s))$, but leaving s_i and s_f fixed. This imposes the conditions

$$\bar{u}(u,s_i) = u_i, \quad \bar{u}(u,s_f) = u_f,$$
$$\bar{s}(s_i) = s_i, \quad \bar{s}(s_f) = s_f.$$

All of the terms in the exponential are invariant under the transformation. For example, the term

$$\int_{s_i}^{s_f} ds\, \mathbf{p}(s) \cdot \frac{\partial \hat{\beta}(s)}{\partial s}$$

becomes

$$\int_{s_i}^{s_f} d\bar{s}\, \frac{ds}{d\bar{s}}\, \mathbf{p} \cdot \frac{\partial \hat{\beta}}{\partial \bar{s}}\, \frac{d\bar{s}}{ds} = \int_{s_i}^{s_f} ds\, \mathbf{p} \cdot \hat{\beta},$$

and so is invariant. Similarly, the remaining two terms are invariant if

$$\frac{|\dot{\mathbf{x}}_\perp|}{\hat{\beta} \cdot \hat{\mathbf{n}}_S} = \frac{d\bar{s}}{ds} \frac{|\dot{\bar{\mathbf{x}}}_\perp|}{\hat{\beta} \cdot \hat{n}_S}.$$

To show that this is the case, note that we can write

$$\dot{\mathbf{x}} = \frac{d\bar{s}}{ds}[\dot{\bar{\mathbf{x}}} + K^a \bar{\mathbf{x}}_a],$$

where

$$K^a = \frac{ds}{d\bar{s}} \frac{\partial \bar{u}^a}{\partial s}.$$

Using $\bar{\mathbf{x}}_a$ and $\dot{\bar{\mathbf{x}}}$, f^a can be written

$$f^a = \frac{d\bar{s}}{ds} \Lambda_b^a (\bar{f}^b + K^b),$$

with

$$\bar{f}^a = \bar{g}^{ab}(\dot{\bar{\mathbf{x}}} \cdot \bar{\mathbf{x}}_b).$$

Combining these expressions to construct $\dot{\mathbf{x}}_\perp$, the dependence on K^a cancels, and we have

$$\dot{\mathbf{x}}_\perp = \frac{d\bar{s}}{ds} \dot{\bar{\mathbf{x}}}_\perp.$$

Since $\dot{\mathbf{x}}_\perp$ is parallel to the surface normal in both coordinate systems, the normal is invariant, and we have the result that τ_{eff} is invariant under local coordinate transformations.

From the expression for the measure, (Du) transforms as

$$(Du) \to (D\bar{u}) \prod \det(\Lambda),$$

while the determinant becomes

$$\text{Det}\left(\frac{\partial}{\partial s}\right)^2 \to \prod \left|\frac{ds}{d\bar{s}}\right|^{-2} \text{Det}\left(\frac{\partial}{\partial \bar{s}}\right)^2.$$

The delta function argument transforms as [using the fact that $\dot{\bar{\mathbf{x}}}_\perp = (ds/d\bar{s})\dot{\mathbf{x}}_\perp$]

$$\dot{u}^a - (\mathbf{x}^a \cdot \hat{\beta}) \frac{|\dot{\mathbf{x}}_\perp|}{\hat{\beta} \cdot \hat{n}_S} + f^a = \frac{d\bar{s}}{ds} \Lambda_a^b \left\{ \bar{u}^a - (\bar{\mathbf{x}}^a \cdot \hat{\beta}) \frac{|\dot{\bar{\mathbf{x}}}_\perp|}{\hat{\beta} \cdot \bar{n}_S} + \bar{f}^a \right\},$$

so that the delta function constraint becomes

$$\prod \det(\Lambda^{-1}) \prod \left|\frac{ds}{d\bar{s}}\right|^2 \prod \delta\left(\bar{u}^a - (\bar{\mathbf{x}}^a \cdot \hat{\beta}) \frac{|\dot{\bar{\mathbf{x}}}_\perp|}{\hat{\beta} \cdot \bar{n}_S} + \bar{f}_a\right).$$

The $\det(\Lambda)$ and $\Pi|ds/d\bar{s}|$ factors in the delta function, determinant, and measure transformations cancel each other, leaving Eq. (12) invariant under transformations of the imbedded surface parametrization.

Invariance under local coordinate transformations is a generalization of the invariant imbedding principle, in that the imbedded surfaces can be arbitrary shape without altering the evolution operator.

VI. NUMERICAL CONSIDERATIONS

The geometrical formalism and invariant imbedding results described above potentially can influence the design of numerical algorithms and codes for integrating the radiative transfer equation. The purpose of this section is to speculate on avenues of exploiting these geometrical results in numerical schemes. We exclude from the discussion algorithms that explicitly trace ray paths through the entire medium, such as Monte Carlo algorithms, because it is not necessary to include geometry in them as we have done here.

An important class of numerical schemes are finite-difference methods such as those presented in Refs. 20 and 21. Such methods in fully three-dimensional problems are generally best suited for rectilinear geometries because the finite differences are along Cartesian coordinate axes. More complicated boundaries are handled by using a rectilinear grid of spatial points with sufficient resolution to include the desired features. However, if these schemes could be written in terms of finite differences in the (u,s) variables, i.e., by the replacement

$$\nabla \rightarrow \frac{\hat{n}_s}{|\dot{\mathbf{x}}_\perp|}\frac{\partial}{\partial s}+\left(\mathbf{x}^a - f^a\frac{\hat{n}_s}{|\dot{\mathbf{x}}_\perp|}\right)\frac{\partial}{\partial u^a},$$

two possible advantages may be realized. The first is that the boundary conditions are easier to specify on the spatial grid, since the boundaries correspond to $s=$ const. The second could occur when the number of spatial points in a calculation exceeds the capacity of the computer core memory. In this situation a large fraction of the total execution time can be spent swapping portions of the spatial grid in and out of the core (the I/O operation is the slowest operation in many computers). However, in a geometrical formulation, the spatial grid could be replaced by a single set of points $\{u_i\}$ on the u plane, and points in space generated by a mapping formula for each surface. The time spent in I/O operations would be replaced by time for calculation of the geometric quantities, such as the metric, on the surfaces. The second potential advantage should be realizable when the total computational time for repeatedly executing a mapping formula is less than the total I/O transfer time for swapping grid points in and out of the core. The balance between these two approaches would depend on the machine, as well as on the particular geometry under consideration. This time-savings argument may be valid for other numerical schemes, also.

One possible numerical algorithm which is different from the typical finite-difference algorithms, yet has a similar structure, is based on the interaction principle in Eq. (2). Changing notation somewhat, Eq. (1) can be written

$$L(u,s,\hat{n}) = \int d^2u'\, d\Omega'\, G(u,s,\hat{n};u',s_i,\hat{n}') \times L(u',s_i,\hat{n}').$$

Using the interaction principle in its iterated form, we obtain the finite-difference equation for the distribution at s_j in terms of the distribution at s_{j-1}:

$$L(u,s_j,\hat{n}) = \int d^2u'\, d\Omega'\, G(u,s_j,\hat{n};u',s_{j-1},\hat{n}') \times L(u',s_{j-1},\hat{n}'). \tag{13}$$

This solution has the form of a finite difference. A numerical algorithm would follow if a suitable discretization scheme can be found. In fact, Eq. (13) is analogous to the starting point of a finite-difference algorithm constructed for time-dependent radiative transfer,[14] and the discretization steps used in that case can be applied to this problem as well. Those steps, as applied to this current problem, are summarized below.

The first step is to discretize the angular degrees of freedom by introducing a set of directions $\{\hat{n}_k\}$, $k=1,\ldots,N$, which point in the directions of the centroids of a set of solid angles $\{\Delta\Omega_k\}$. Defining the averaged radiance

$$L_k(u,s) = \int_{\Delta\Omega_k} d\Omega\, L(u,s,\hat{n})\Delta\Omega_k,$$

the angularly discretized finite difference equation is

$$L_k(u,s_j) = \sum_{k'}\int d^2u'\, G_{kk'}(u,s_j;u',s_{j-1}) \times L_{k'}(u',s_{j-1}),$$

where

$$G_{kk'}(u,s;u',s') = \frac{1}{\Delta\Omega_k}\int_k d\Omega \int_{k'} d\Omega' \times G(u,s,\hat{n};u',s',\hat{n}')$$

is the discretized version of the evolution operator.

The next step is to construct $G_{kk'}$ in terms of the discretized phase function. This will require the interpretation of the difference $s_j - s_{j-1} = ds$ as a small quantity. The precise criterion for smallness follows from examining the magnitude of the higher-order terms excluded in the approximation. In analogy with the time-dependent case, the criterion is essentially $b\, ds|\dot{\mathbf{x}}_\perp| < 1$, i.e., that the propagation distance between adjacent surfaces is less than a single scattering length. Assuming ds is small, we can use Eqs. (9) and (11) to write an approximate discretization (see Ref. 12 for the full derivation)

$$G_{kk'}(u,s+ds;u',s) = \delta(u^a - u'^a - du^a_{k'}(s,u))\exp\{-c\, dl(u,s,\hat{n}_{k'})\} \times (\exp\{b\,|\dot{\mathbf{x}}_\perp|(u,s)|ds\,\mathbf{Q}\})_{kk'},$$

where

$$du^a_k(s,u) = ds\left\{(\mathbf{x}^a(u,s)\cdot\hat{n}_k)\frac{|\dot{\mathbf{x}}_\perp(u,s)|}{\hat{n}_k\cdot\hat{n}_S(u,s)} - f^a(u,s)\right\},$$

$\mathbf{Q}$ is the matrix with elements

$$Q_{kk'} = P_{kk'}/\hat{n}_{k'}\cdot\hat{n}_S(u,s),$$

and $\mathbf{P}$ is

$$P_{kk'} = \frac{1}{\Delta\Omega_k}\int_k d\Omega \int_{k'} d\Omega'\, P(\hat{n}\cdot\hat{n}').$$

This method of discretizing the phase function has been used in both time-independent[20,22] and time-dependent[14] radiative transfer.

Assembling these steps, the numerical algorithm is the explicit finite-difference formulation

$$L_k(u,s+ds) = \sum_{k'}\exp\left\{-c|\dot{\mathbf{x}}_\perp|\frac{ds}{\hat{n}_{k'}\cdot\hat{n}_S}\right\} \times \exp\{b\,|\dot{\mathbf{x}}_\perp|ds\,\mathbf{Q}\}_{kk'}L_{k'}(u-du_{k'},s).$$

In this form the computationally intensive elements of the algorithm are the exponentiation of the matrix and the spatial interpolations needed to estimate the distribution at the points $u - du_k$.

An alternative discretization is to expand in spherical harmonics, so that the elements of the matrix $\mathbf{Q}$ are obtained from the spherical harmonics expansion for P and $\hat{n}$. The numerical algorithm would follow by truncating the expansion to some finite number of harmonics, and exponentiating $\mathbf{Q}$ as before. The utility of each of these two methods of discretization should depend on the structure of the phase function and on the angular resolution necessary for a specific calculation, although this issue has not been examined in detail.

The primary test of the utility of any algorithm based on geometric methods, however, will be the actual construction and execution of a code to determine directly its computational resource usage.

VII. CONCLUSIONS

The path integral solution of the radiative transfer equation has been constructed for problems involving curved or irregular boundaries in a medium. Several concepts and quantities from differential geometry have been used to make the solution compact. The path integration is over paths through the surfaces intermediate (imbedded) between the initial and final surfaces. The principle of invariant imbedding is satisfied by this solution, in the form of explicit invariance of the path integral to local coordinate transformations of the imbedded surfaces. It is hoped that this form of invariant imbedding can be exploited efficiently in a numerical algorithm and code. Existing and new numerical algorithms could incorporate this geometrical formulation to exploit its convenient parametrization of boundaries, and possibly to save execution time in calculations involving large numbers of spatial points.

ACKNOWLEDGMENT

This work was partly supported by NASA Contract No. NAG5-869.

[1]J. Simpson, R. F. Adler, and G. R. North, "A proposed tropical rainfall measuring mission (TRMM) satellite," Am. Meterol. Soc. **69**, 278 (1988).

[2]J. A. Weinman and P. J. Guetter, "Determination of rainfall distributions from microwave radiation measured by the Nimbus 6 ESMR," J. Appl. Meterol. **16**, 437 (1977); R. W. Spencer, B. B. Hinton, and W. S. Olson, "Nimbus-7 37 GHz radiances correlated with radar rain rates over the Gulf of Mexico," J. Cli. Appl. Meterol. **22**, 2095 (1983); R. W. Spencer, "A satellite passive 37-GHz scattering-based method for measuring oceanic rain rates," J. Cli. Appl. Meterol. **25**, 754 (1986).

[3]J. A. Weinman and R. Davies, "Thermal microwave radiances from horizontally finite clouds of hydrometeors," J. Geophys. Res. **83** (C6), 3099 (1978); C. Kummerow and J. A. Weinman, "Determining microwave brightness temperatures from precipitating horizontally finite and vertically structured clouds," *ibid.* **93** (D4), 3720 (1988).

[4]T. B. McKee and S. K. Cox, "Scattering of visible radiation by finite clouds," J. Atmos. Sci. **31**, 1885 (1974); M. Aida, "Scattering of solar radiation as a function of cloud dimensions and orientation," J. Quant. Spectrosc. Radiat. Transfer **17**, 303 (1980).

[5]R. W. Preisendorfer and G. L. Stephens, "Multimode radiative transfer in finite optical media. I: Fundamentals," J. Atmos. Sci. **41**, 709 (1984); G. L. Stephens and R. W. Preisendorfer, "Multimode radiative transfer in finite optical media. II: Solutions," J. Atmos. Sci. **41**, 725 (1984); G. L. Stephens, "Radiative transfer through arbitrarily shaped optical media. Part I: A general method of solution," *ibid.* **45**, 1818 (1988); G. L. Stephens, "Radiative transfer through arbitrarily shaped optical media. Part II: Group theory and simple closures," *ibid.* **45**, 1837 (1988).

[6]N. Witherspoon, M. Strand, J. Holloway, B. Price, D. Brown, R. Mill, and L. Estrup, "Experimentally measured MTFs associated with imaging through turbid water," SPIE J. **925**, (Ocean Optics IX), 363 (1988).

[7]W. H. Wells, "Loss of resolution in water as a result of multiple small-angle scattering," J. Opt. Soc. Am. **59**, 686 (1969).

[8]J. S. Jaffe and C. Dunn, "A. model-based comparison of underwater imaging systems," SPIE J. **925** (Ocean Optics IX), 344 (1988).

[9]R. W. Preisendorfer, *Radiative Transfer on Discrete Spaces* (Pergamon, New York, 1965).

[10]G. W. Kattawar, J. Quant. Spectrosc. Radiat. Transfer **13**, 145 (1973).

[11]R. W. Preisendorfer, *Hydrologic Optics* (Pacific Marine Environmental Laboratory, ERL/NOAA, Honolulu, 1976), Vol. 11.

[12]J. Tessendorf, "Radiative transfer as a sum over paths," Phys. Rev. A **35**, 872 (1987).

[13]P. J. Flatau and G. L. Stephens, "On the fundamental solution of the radiative transfer equation," J. Geophys. Res. **93** (D9), 11037 (1988); P. C. Waterman, "Matrix-exponential description of radiative transfer," J. Opt. Soc. Am. **71**, 410 (1981).

[14]J. Tessendorf, "Time-dependent radiative transfer and pulse evolution," J. Opt. Soc. Am. A **6**, 280 (1989); J. Tessendorf, C. Piotrowski, and R. L. Kelly, "Finite-difference evolution of a scattered laser pulse in ocean water," SPIE J. **925** (Ocean Optics IX), 22 (1988).

[15]J. Tessendorf, "Comparison between data and small-angle approximations for the in-water solar radiance distribution," J. Opt. Soc. Am. A **5**, 1410 (1988).

[16]R. S. Millman and G. D. Parker, *Elements of Differential Geometry* (Prentice–Hall, Englewood Cliffs, NJ, 1977).

[17]L. S. Dolin, Izv. Atmos. Oceanic Phys. **16**, 34 (1980).

[18]L. D. Faddeev and V. N. Popov, "Feynman diagrams for the Yang–Mills field," Phys. Lett. B **25**, 29 (1967).

[19]H. M. Fried and J. Tessendorf, "Green's functions at zero viscosity," J. Math. Phys. **25**, 1144 (1984).

[20]W. S. Helliwell, "Finite-difference solution to the radiative-transfer equation for in-water radiance," J. Opt. Soc. Am. A **2**, 1325 (1985).

[21]R. D. Richtmyer and K. W. Morton, *Difference Methods for Initial-Value Problems* (Interscience, New York, 1967).

[22]C. D. Mobley and R. W. Preisendorfer, "A numerical model for the computation of radiance distributions in natural waters with wind-roughened surfaces," NOAA Technical Memorandum ERL PMEL-75, 1988.